Aquaculture International (2025) 33:508
https://doi.org/10.1007/s10499-025-02192-5

RESEARCH

Transcriptomic analysis of leukocyte immunometabolic dynamics in hemorrhagic sepsis in *Piaractus mesopotamicus*

Gustavo S. Claudiano[1,2,3] · Larissa A. F. Sampaio[1] · Sónia C. S. Andrade[4] · Elaine C. Souza[5] · Jefferson Yunis-Aguinaga[8] · Paulo F. Marcusso[6] · Juliana N. Ferreira[2] · Andrya L. Leão[1] · Thayná M. dos Santos[1] · Layana A. B. Pereira[2] · Laine P. C. dos Santos[2] · Luiz L. Coutinho[7] · Cleni M. Marzocchi-Machado[9] · Julieta R. E. Moraes[3,10]

Received: 23 June 2025 / Accepted: 7 August 2025

Abstract
Sepsis caused by *Aeromonas hydrophila* in *Piaractus mesopotamicus* triggers a complex transcriptomic reprogramming in circulating leukocytes. This study employed RNA-Seq to profile temporal changes in gene expression during the early stages of sepsis (1, 3, 6, and 9 h post-infection, HPI). A total of 17,698 differentially expressed genes (DEGs) were identified, with transcriptional peaks at 3 and 9 HPI. Functional classification (KOG) revealed enrichment in genes related to energy metabolism, amino acid metabolism, and protein synthesis. Gene Ontology (GO) and KEGG pathway analyses showed that leukocytes preferentially activated pathways involved in anaerobic glycolysis, the Krebs cycle, and lipid metabolism—particularly steroid hormone biosynthesis. Key immunometabolic pathways, including PI3K-AKT, mTOR, and TLR signaling, were dynamically modulated, indicating their role in maintaining ionic balance and promoting leukocyte survival during systemic inflammation. In addition, substantial reprogramming of iron and calcium metabolism was observed, suggesting a host strategy to limit bacterial growth by restricting access to essential micronutrients. These metabolic shifts correlated with disease severity, as evidenced by the high mortality rate (71.4% at 120 HPI) and pronounced histopathological damage in vital organs. Altogether, these findings demonstrate that leukocytes initiate a robust but potentially deleterious immunometabolic response to *A. hydrophila*, contributing both to host defense and to tissue injury. This work provides valuable molecular insights into the pathogenesis of septicemia in fish and offers a foundation for developing targeted strategies to mitigate Aeromonosis in aquaculture.

Keywords Aeromonosis · RNA-Seq · Teleosts · Energy metabolism · Immunity · Inflammation

Handling Editor: Amany Abbass

Extended author information available on the last page of the article

Introduction

Sepsis, a life-threatening systemic inflammatory response to infection, represents a significant challenge in both human and veterinary medicine, with *Aeromonas hydrophila* being a prominent causative agent in aquatic species (Ahmed et al. 2018; Marinho-Neto et al. 2019). This pathogen is particularly detrimental in aquaculture, where it causes high morbidity and mortality, leading to substantial economic losses. Despite advancements in understanding the pathophysiology of sepsis and the development of therapeutic strategies, critical challenges remain, including the need for early diagnostic markers, a deeper understanding of molecular mechanisms, and more effective treatment options (Goris 1996; Lévy et al. 2012). The progression of sepsis is characterized by a dysregulated immune response, marked by an imbalance between pro- and anti-inflammatory processes, which can result in severe tissue damage, immunosuppression, and multi-organ failure (Levy et al. 2003; Hotchkiss et al. 2013).

Blood leukocytes, including lymphocytes, granulocytes, monocytes, and thrombocytes, undergo significant transcriptional and functional changes during sepsis. These cells play a pivotal role in orchestrating the immune response through mechanisms such as cytokine release, phagocytosis, and direct pathogen interaction (Claudiano et al. 2019, 2020). In teleost fish, leukocytes are particularly crucial for managing systemic infections, as they mediate both the initial containment and the sustained inflammatory response against pathogens like *A. hydrophila* (Yunis-Aguinaga et al. 2016; Claudiano et al. 2019; Marinho-Neto et al. 2019). Thrombocytes, often overlooked in other species, have been shown to contribute significantly to immune defense in fish, participating in phagocytosis, pathogen interaction, and modulation of inflammatory and hemostatic responses (Tavares-Dias 2006, Tavares-Dias and Moraes 2007, Claudiano et al. 2019).

The complexity of sepsis necessitates advanced molecular tools to dissect the intricate cellular and molecular changes occurring during infection. RNA sequencing (RNA-Seq) has emerged as a powerful technique for profiling gene expression, offering insights into the transcriptional landscape of immune cells under pathological conditions. However, the high abundance of globin transcripts from erythrocytes can obscure leukocyte-specific signals, necessitating strategies such as globin RNA depletion to enhance the sensitivity and accuracy of transcriptomic analyses (Debey et al. 2004; Fan and Hegde 2005; Talwar et al. 2006; Ronza et al. 2021).

RNA-Seq enables a comprehensive exploration of the transcriptional, metabolic, and immunological alterations that occur during sepsis, facilitating the identification of key molecular pathways and genes involved in disease pathogenesis. Such insights are invaluable for developing targeted therapeutic and prophylactic strategies (Yang et al. 2016; Mastrochirico-Filho et al. 2020; Xiong et al. 2022).

In this study, we aimed to characterize the global transcriptomic response of blood leukocytes in *Piaractus mesopotamicus* during *A. hydrophila*–induced sepsis. By analyzing gene expression profiles at multiple time points post-infection, we sought to elucidate the molecular mechanisms underlying the immune, metabolic, and energetic adaptations of leukocytes during sepsis. Furthermore, this study establishes a foundational transcriptomic resource for *P. mesopotamicus*, offering critical insights for improving diagnostic, prophylactic, and therapeutic approaches in aquaculture.

Materials and methods

Fish and bacterial strain

Fifty-five pacu (*Piaractus mesopotamicus*; 180.7 ± 38.1 g, 21.3 ± 6.7 cm) were initially acclimated together for 7 days in three 5000-L outdoor tanks. Subsequently, they were randomly distributed into eleven 250-L fiber boxes (5 fish per box), all receiving artesian well water (1 L/min) under continuous aeration via a shared recirculation system to ensure a uniform microenvironment. The fish were fed a commercial diet (3% biomass, 28% crude protein, and 4000 kcal of gross energy per kg). The study was conducted in compliance with Brazilian animal welfare guidelines and ISO standards (International Organization for Standardization 2006) and was approved by the Ethics Committee (Approval No. 008577/12). Water quality parameters were maintained within optimal ranges for pacu throughout the experiment: dissolved oxygen = 5.3 mg/L, temperature = 8.87 °C, pH = 7.53, and electrical conductivity = 118.26 µS/cm (Boyd 1990).

Aeromonas hydrophila strain was isolated from naturally infected fish that presented lesions compatible with Aeromonosis (Marinho-Neto et al. 2019). After euthanasia by deep anesthesia in 1:10.000 aqueous solution of benzocaine. Fish were necropsied and fragments of the brain, kidney, and blood were aseptically sampled for bacteriological culture. The initial identification of colonies was performed according to Abeyta et al. (1990) supplemented by biochemical proofs made by means of the commercial kit (Bactray 3 Laborclin®), according to the manufacturer recommendations. For genetic characterization, the bacterial mass derived from pure colonies culture was submitted to a DNA extraction process, according to the manufacturer's suggested methodology (Genomic DNA Purification Kit Wizard®). DNA concentration was 1690.9 ng/µL, with ratio 260/280 and 260/230, 2.02, and 2.04, respectively. After obtaining the DNA, ribosomal gene 16 S RNA (forward primer AACCTGGTTCCGCTCAAGCCGTTG and reverse primer TTG CCTCGCCTCGGCCCAGCAGCT) was amplified according to Sarkar et al. (2012) and followed sequencing (Marinho-Neto et al. 2019).

The pathogenicity of strain of *A. hydrophila* was verified by three serial passages and re-isolation was performed in pacus, which were in oculated with 1.0 mL of bacterial suspension (2.4×10^8 CFU/mL) by coelom via. After the third passage, the bacteria re-isolated from fish tissue underwent the same tests of microbial and molecular confirmation described above (Claudiano et al. 2019).

Induction of sepsis and collection of blood

Sepsis was induced by intraperitoneal injection of 0.5 mL of a bacterial inoculum at a concentration of 1.8×10^8 CFU/mL, corresponding to the 50% lethal dose (LD_{50}) (Claudiano et al. 2019). Prior to injection, the fish were anesthetized using a benzocaine solution (1:20,000) diluted in 98% ethanol (0.1 g/mL) until reaching a surgical anesthesia according to Ross and Ross (2008). The fish were randomly distributed into two groups: a control group injected with 0.5 mL of sterile 0.65% sodium chloride solution and a challenged group injected with the same volume of sodium chloride solution containing the bacterial inoculum (Marinho-Neto et al. 2019).

For the experiment, fish ($n = 8$ per time point) were euthanized by deep anesthesia at 1, 3, 6, and 9 h post-infection (HPI), along with the control group. Peripheral blood samples

were collected by caudal venipuncture using a sterilized hypodermic syringe, obtaining a final volume of 1.0 mL of blood per sample (Claudiano et al. 2020).

Total RNA extraction and data analyses

Optimization of total RNA extraction

Blood samples were collected in pre-chilled microtubes, flash-frozen in liquid nitrogen, and maintained on ice until processing. Total RNA extraction was optimized using nine fish distributed into three groups ($n = 3$ per group) in 250-L tanks in duplicate. The groups were randomized as follows: G1: Illustra RNAspin Mini Kit™ (GE Healthcare®), G2: RNeasy Mini Kit (Qiagen®), and G3: Trizol reagent (Invitrogen®) followed by purification using the RNeasy Mini Kit (Qiagen®). The processing was carried out according to the manufacturer's recommendations.

To eliminate genomic DNA contamination, all samples were treated with DNase I (Qiagen®) for 1 h during purification. RNA concentration and purity were quantified using a NanoDrop ND-1000 spectrophotometer (Thermo Fisher Scientific Inc.). Samples with RNA concentrations ≥ 100 ng/µL were further analyzed for integrity using an Agilent 2100 Bioanalyzer (Agilent RNA 6000 Nano Kit).

Total RNA extraction from blood leukocytes

Total RNA was extracted from blood collected at the designated time points using the optimized protocol (G3). Blood samples were collected in 15-mL Falcon tubes (Corning®) containing Trizol reagent (Invitrogen®) and maintained on crushed ice. RNA extraction was performed using the Trizol method, with 0.75 mL of reagent per 0.25 mL of blood, followed by purification with the RNeasy Mini Kit (Qiagen®). Samples were treated with RNase-Free DNase Set (Qiagen®) for 1 h at room temperature. RNA concentration and purity were quantified using a NanoDrop ND-1000 spectrophotometer, while DNA contamination was assessed using the Qubit® RNA HS Assay Kit (Invitrogen®) and Qubit dsDNA HS Assay Kit (Life Technologies®). RNA integrity was evaluated using the Agilent 2100 Bioanalyzer (Agilent RNA 6000 Nano Kit).

cDNA library construction and sequencing

Twenty RNA samples (five per timepoint: 0, 1, 3, 6, and 9 HPI) with RIN > 8 were selected for library construction using the TruSeq Stranded Total RNA with Ribo-Zero Globin Set B kit (Illumina). This kit employs biotinylated probes and magnetic beads to deplete cytoplasmic and mitochondrial rRNA plus globin mRNA in a single step, while preserving strand specificity and capturing both coding and noncoding transcripts. Libraries were prepared from 0.1 to 1 µg input RNA following the manufacturer's protocol (fragmentation, first- and second-strand cDNA synthesis, end repair, A-tailing, adapter ligation, and PCR enrichment) and sequenced on an Illumina HiSeq 2500 with 100 bp paired-end reads.

Raw sequencing data were processed using CASAVA v1.8.2 (Illumina®). Low-quality reads, primer sequences, and vector contaminants were removed using Seqyclean v1.9.10 with a quality cutoff of Q24 and reference to the UniVec database. Reads shorter than 65 bp were discarded. Filtered reads were normalized using the Trinity v2.0.6 package, which was also used to assemble the reference transcriptome. Assembly quality was

evaluated based on average contig length (2695 bp), N50, and functional annotation coverage. Coding sequences were identified using BLASTX (e-value cutoff of 1e-5) against the Swiss-Prot database. Read mapping was performed with Bowtie2 v2.2.6, and differential gene expression analysis was conducted using edgeR (v3.X). DEGs were identified using a negative binomial model with Benjamini–Hochberg correction for multiple testing. Genes with FDR < 0.05 and $|\log_2$ fold change$| \geq 1$ were considered significantly differentially expressed. Immune-related DEGs were selected based on their annotation and cross-referencing with the InnateDB database (www.innatedb.com), which compiles genes empirically linked to innate immune responses.

GO and KEGG enrichment analyses were performed using Fisher's exact test with the Benjamini–Hochberg correction for multiple testing. Enriched terms were considered significant at FDR < 0.05. Additionally, the Functional Classification of Leukocyte Transcripts was performed using KOG (Tatusov 2000).

All processed RNA-Seq data used in the analyses, including DEGs and enrichment results, are provided as supplementary material (Tables S1–S4). GO and KEGG analyses were conducted to annotate DEGs and identify enriched pathways (Tatusov et al. 2003).

Bacterial quantification and mortality assay

Bacterial load in blood was quantified by culturing 20 µL of whole blood from challenged and control groups on tryptic soy agar (TSA) supplemented with ampicillin (10 mg/L). Plates were incubated at 30 °C for 24 h, and *A. hydrophila* colonies were enumerated and characterized.

A mortality assay was conducted using 56 pacu divided into two groups: one injected with 0.5 mL of *A. hydrophila* suspension (1.8×10^8 CFU/mL) and the other with 0.5 mL of sterile saline (0.65%). Mortality was monitored at 1, 3, 6, 9, 12, 18, 24, 36, 48, 72, 96, and 120 HPI. The lethality index (%) was calculated as follows:

$$\text{Lethality Index}(\%) = (\text{Cumulative deaths}/\text{otal individuals challenged}) \times 100$$

Results

Optimization of total RNA extraction

In the optimization of total RNA extraction, the combined Trizol + RNeasy Mini Kit protocol (TM3) achieved a mean yield of 144 ng/µL and high integrity (RIN 8.0–9.1), whereas TM1 yielded only ~ 3 ng/µL with undetectable RIN and TM2 yielded ~ 2.3 ng/µL (Qiagen) or ~ 98 ng/µL (GE) with low integrity (RIN 2.5). Based on these results, TM3 was adopted for all subsequent RNA-Seq extractions.

Transcriptome features

Sequencing of the blood leukocyte transcriptome during *Aeromonas hydrophila*–induced sepsis in *Piaractus mesopotamicus* generated 266,272 high-quality reads after filtering, with most contigs exceeding 999 bp (mean length: 25,695 bp; Table 1). Comparative analysis revealed significant temporal regulation, with the highest number of

Table 1 Description of the transcriptome of *P. mesopotamicus*

	N of contigs
Total number of contigs	**266,272**
Total contigs analized	252,535
299–499 pb	81,038
500–999 pb	51,893
>999 pb	119,604
N50	2786
Minimum contig length (pb)	299
Maximum contig length (pb)	120,230
Total transcripts	19,595
Control	7160
1 HPI	1775
3 HPI	4999
6 HPI	2179
9 HPI	3482
Total contigs (CxT)	
cx1 hpi	44,453
cx3 hpi	41,543
cx6 hpi	46,187
cx9 hpi	44,154
Enrichment analysis	
Gene Ontology (seqs)	
Molecular function	45,726
Cellular component	26,126
Biological process	54,379
KEGG (pathway)	120
COG (seqs)	15,000

N50 – statistically weighted average such that 50% of the entire assembly is formed by contigs of equal size or larger than this value. Minimum and Maximum, respectively, size of the shortest and largest contigs obtained in the respective assembly. *Seqs*, genetic sequence; *KEGG*, Kyoto Encyclopedia of Genes and Genomes; *KOG*, EuKaryotic Orthologous Groups; *HPI*, hours after infection; *N*, number

differentially expressed genes (DEGs) at 3 and 9 h post-infection (HPI) (Fig. 1A). Venn diagrams demonstrated 7097 genes exclusively expressed in controls, while infection induced time-specific responses: 442 (1 HPI), 2417 (3 HPI), 369 (6 HPI), and 1088 DEGs (9 HPI) (Fig. 1B). Upregulation peaked at 3 HPI (4999 genes), while downregulation dominated at 9 HPI (3860 genes) (Fig. 1C, D), with 27.2% upregulated and 21.2% downregulated genes shared between these timepoints (Supplementary Table S1 (Excel file) and Supplementary Table S2).

Enrichment analysis of the septic pacu leukocyte transcriptome (Table 1) revealed that the majority of sequences were associated with biological processes (45,726), followed by molecular functions (45,726) and cellular components (26,126) (Supplementary Table S3). Kyoto Encyclopedia of Genes and Genomes (KEGG) analysis identified 896 enzymes participating in 120 distinct metabolic pathways in septic leukocytes (Supplementary Table S4). Additionally, Clusters of Orthologous Groups (COG) database

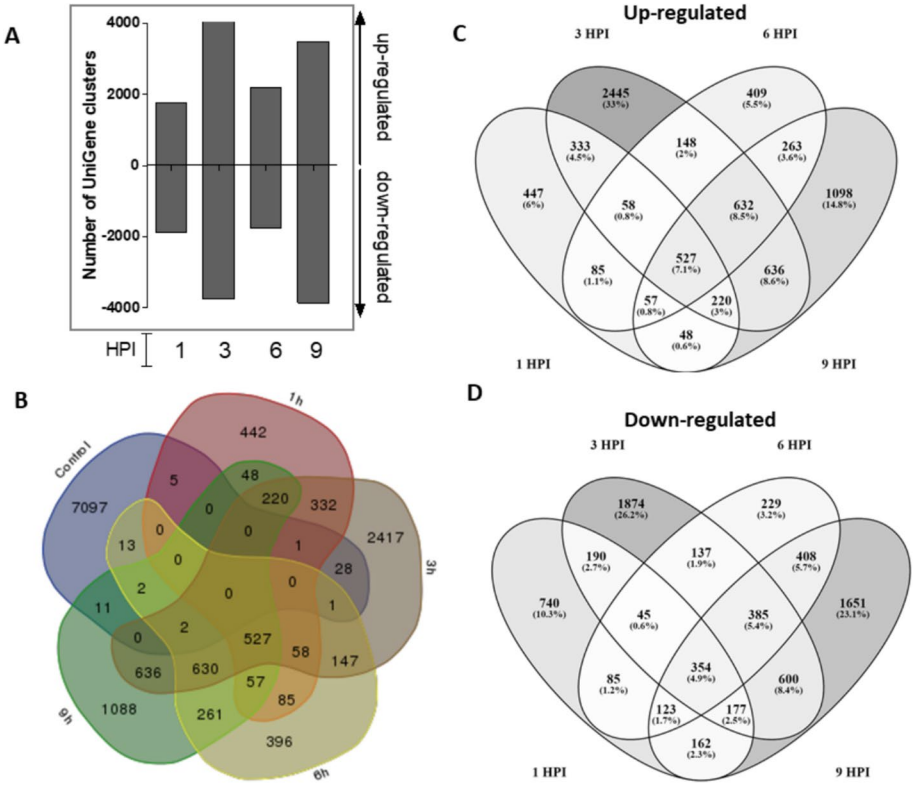

Fig. 1 **A** Number of differentially expressed UniGene clusters over the experimental time. **B** Venn diagram showing the overlap of upregulated genes among the time points. **C** Overlap of downregulated genes across the different time points. **D** Comparison among the experimental time points highlighting the upregulated genes

analysis annotated 15,000 unigenes, classifying them into 26 functional categories (Table 1).

Profile of genes expressed by leukocytes after bacterial challenge: immunity

Genes included in the heatmap were selected based on their known immunological relevance and consistent expression patterns across biological replicates (Fig. 2, Supplementary Table S2). Early infection (1 HPI) was marked by downregulation of inflammatory genes (e.g., interleukins, interferons, TNF receptors) but upregulation of oxidative stress markers (e.g., ROS, lysozyme). The low expression of coagulation-related genes (von Willebrand factor) and cell adhesion molecules (integrins, selectins).

As infection progressed, by 3 HPI, a transitional phase began characterized by moderate upregulation of genes involved in cell migration (leukotriene receptors) and inflammatory metabolism (thromboxane and prostaglandin pathways), along with persistence of genes upregulated at 1 HPI (Fig. 2, Supplementary Table S2).

At 6 HPI, a dramatic shift in gene regulation occurred, marked by upregulation of inflammatory response genes, neutrophil recruitment markers, and oxidative stress

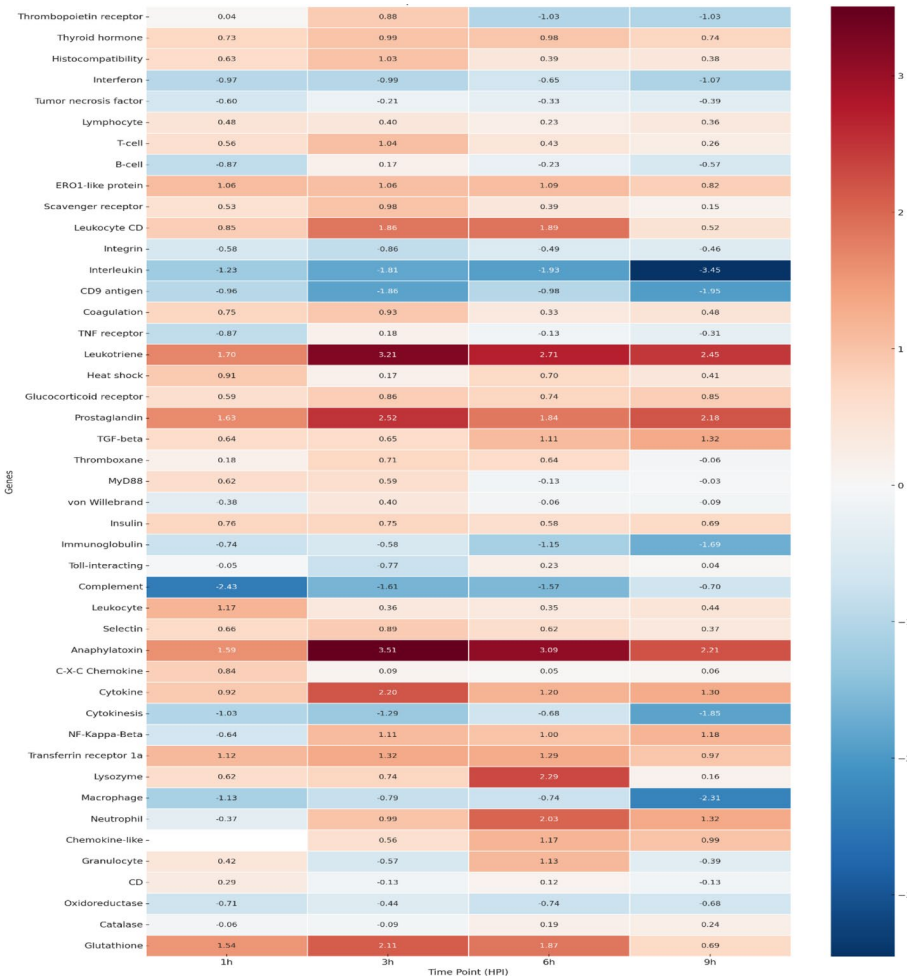

Fig. 2 Heatmap representing the differential expression of immune-related genes in leukocytes of *Piaractus mesopotamicus* during sepsis progression at different post-infection times (1, 3, 6, and 9 hpi). Each row represents a specific gene, while each column corresponds to a time point. Colors indicate the log fold change (FC) in gene expression, with red representing upregulation and blue representing downregulation

pathways (Fig. 2). Elevated expression of heat shock proteins (HSPs), reactive oxygen species (ROS), and transferrin receptors indicated robust ROS production and innate immune activation, characteristic of an exacerbated inflammatory response, concurrently, activation of glucocorticoid and thyroid hormone receptors (Fig. 2).

The peak response (9 HPI) featured cytokine/chemokine induction (TNF-α, IL-1β) and antioxidant activation (catalase, glutathione), alongside recovery of coagulation-related genes (e.g., von Willebrand factor; Supplementary Table S1 (Excel file) and Supplementary Table S2).

Functional classification of transcripts—GO

Gene Ontology (GO) analysis revealed temporal shifts in leukocyte activity (Fig. 3; Supplementary Table S3). During the initial phase (1-h post-sepsis induction), gene expression was predominantly associated with membrane structure (cellular components; Fig. 3). Biological process analysis revealed modulation of serine/threonine kinase activity, accompanied by increased sodium (Na+) and neuropeptide membrane transport, along with activation of Toll-interleukin receptors (TIR) and oxidation–reduction (redox) reactions (molecular functions, MF; Fig. 3). Also, activated leukocytes showed significant alterations in reactive oxygen species (ROS) production, with downregulation of serine/threonine kinase activity and enhanced phagocytosis coupled with hematopoietic stimulation.

By 3 HPI, membrane-associated gene expression became prominent, particularly involving transport complexes (AKTIP/FTS, FAM160A2-Hook proteins) and nuclear structures like the DNA polymerase complex (Fig. 3). Biological processes showed coordinated activation: active membrane transport, mRNA synthesis, and stress response pathways (Fig. 3). Concurrently, programmed cell death (apoptosis/necrosis) increased in leukocytes. Molecular function analysis revealed enhanced directed transport of organic/inorganic cations, neurotransmitters, vitamins, and iron (MF, Fig. 3).

At 6 HPI, leukocytes exhibited continued vesicle trafficking and fusion mediated by Hook protein complexes, along with spliceosomal RNA processing (CC, Fig. 3). Biological processes showed marked alterations in leukocyte activity due to disrupted cellular homeostasis, including oxidative stress responses (redox reactions), pigment-related pathways

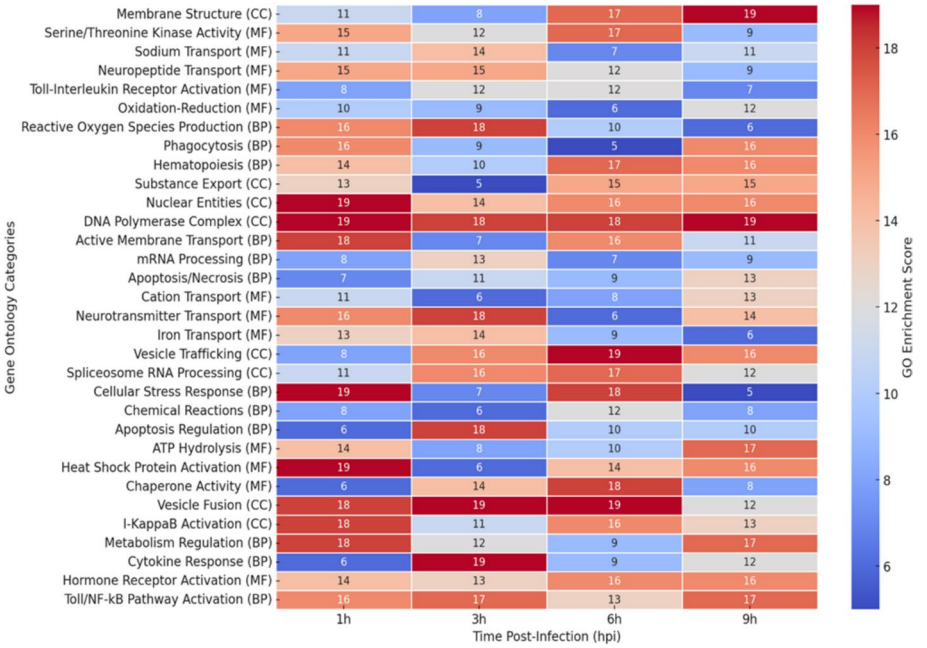

Fig. 3 Gene ontology enrichment analysis of leukocyte transcripts in *P. mesopotamicus* during *A. hydrophyla*–induced sepsis. Cellular component (CC), biological process (BP), and molecular function (MF) identified in pacus

(e.g., melanin synthesis), and enhanced apoptotic regulation (BP, Fig. 3). Molecular functions featured ATP-driven subcellular movement, DNA cleavage activity, and activation of heat shock proteins/chaperones (MF, Fig. 3).

At the final observation timepoint (9 HPI), biological processes dominated the leukocyte transcriptome profile (Fig. 3). Cellular component analysis revealed persistent Hook protein complex-mediated vesicle trafficking and RNA splicing, along with activation of the inhibitory kappaB protein complex (I-κB/IKB; CC, Fig. 3). Biological processes were characterized by metabolic regulation of RNA, macromolecule, and nitrogen biosynthesis, and cell death pathways (BP, Fig. 3). Notably, immune-related processes were prominently upregulated, including cytokine responses (TNF, prostaglandins), hormone/neurotransmitter signaling, and Toll-like receptor/NF-κB activation. Molecular function analysis showed significant cellular activity changes, particularly in hormonal receptor activation and DNA catalytic processes (MF, Fig. 3).

Metabolic pathways in leukocytes during sepsis—KEGG

KEGG analysis revealed that blood leukocytes during *Aeromonas*-induced sepsis undergo significant metabolic reprogramming, with the majority of differentially expressed genes (DEGs) associated with core metabolic functions rather than immune responses (Fig. 4; Supplementary Table S4). Carbohydrate metabolism (24.2%) dominated the transcriptional profile, followed by amino acid (15.07%) and lipid metabolism (10.49%), while

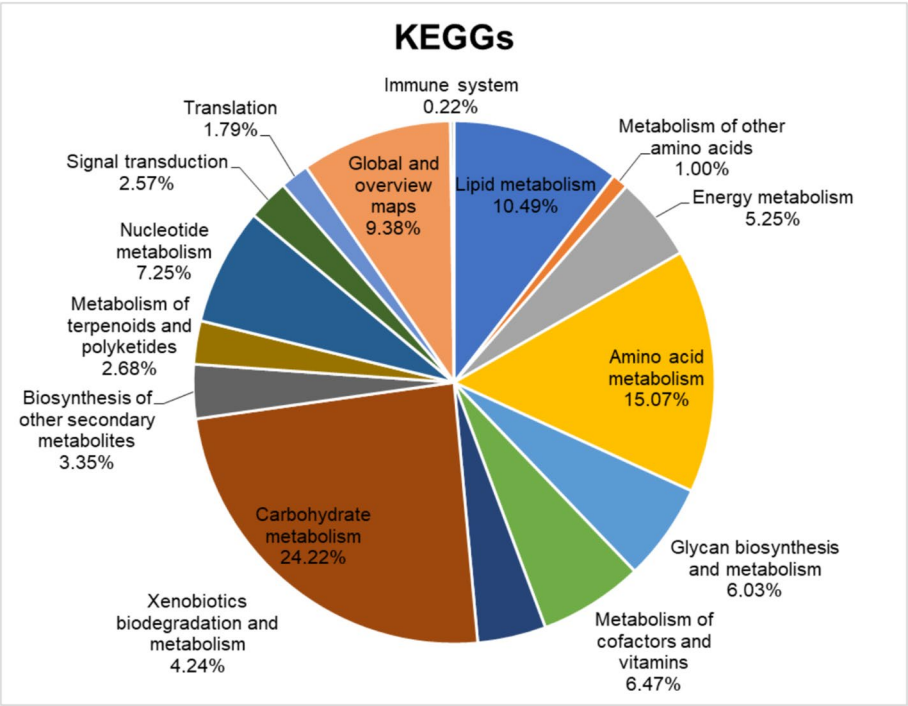

Fig. 4 KEGG pathways obtained from transcripts of leukocytes of *Piaractus mesopotamicus* during *A. hydrophyla*–induced sepsis

immune-related genes represented only 0.22% of DEGs. Early infection triggered anaerobic glycolysis (upregulated *LDHA*) coupled with oxidative pathways (Krebs cycle, oxidative phosphorylation). Iron homeostasis emerged as a key feature, with transferrin receptor (*TFRC*) upregulation indicating leukocyte iron sequestration, linked to amino acid (15.07%) and energy metabolism (5.25%) pathways. Lipid metabolism showed dual regulation of steroid hormone biosynthesis (including cortisol) and arachidonic acid cascades, while xenobiotic degradation pathways (4%) implicated coagulation-related processes.

Parallel signaling analyses (Fig. 5) revealed TLR/NF-κB-driven inflammation, mTOR-mediated cytoskeletal reorganization, phosphatidylinositol-calcium crosstalk maintaining ion homeostasis, and T-cell receptor signaling modulating cytokines (IL-2/4/5/10, IFN-γ, TNF-α).

Functional classification of leukocyte transcripts—KOG

KOG analysis of *Piaractus mesopotamicus* leukocytes during *Aeromonas hydrophila* sepsis demonstrated a functional partitioning dominated by core metabolic processes (energy production [C], amino acid [E], and carbohydrate metabolism [G]), genetic information processing (translation/ribosomal biogenesis [J], DNA replication/repair [L]), and cellular homeostasis (ion transport [P], protein turnover [O, T], transmembrane trafficking [N]) (Fig. 6). While immune regulation genes (V) were identified, their underrepresentation relative to metabolic categories aligns with the metabolic reprogramming observed in pathway analyses. The coordinated upregulation of energy-yielding pathways alongside DNA repair mechanisms.

Lethality index for Aeromonosis

The inoculation of the bacteria in the coelomic cavity allowed its dissemination in the bloodstream of the fish, confirming sepsis by positive blood culture in all challenged groups and negative for fish in the control group. No mortality was observed in the control group. In the challenged group, the first mortality event occurred at 9 HPI, followed

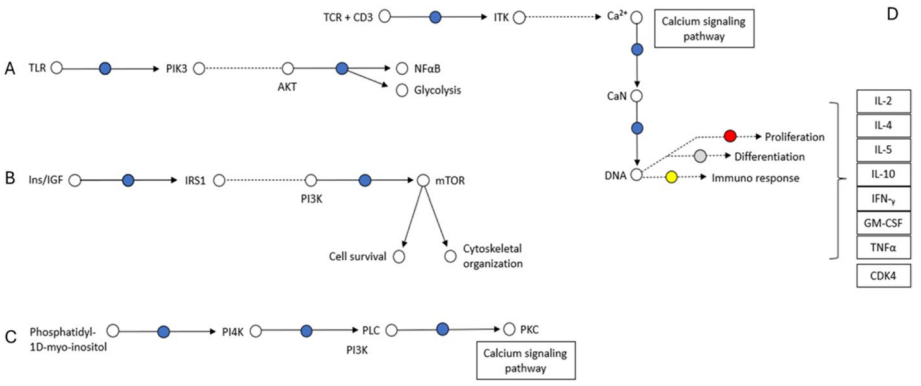

Fig. 5 Signal transduction and immune system pathways from KEGG involved in leukocyte functional reprogramming during sepsis. **A** TLR signaling pathway; **B** mTOR pathway; **C** Phosphatidylinositol e calcium signaling pathways; **D** T-cell receptor signaling pathway

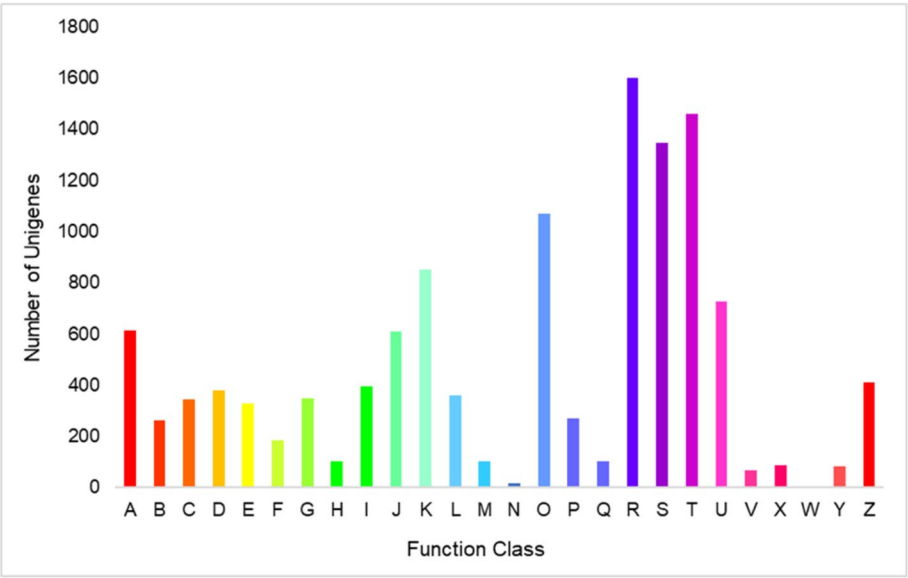

Fig. 6 KOG functional classification of differentially expressed leukocyte transcripts in *Piaractus mesopotamicus* during sepsis induced by *Aeromonas hydrophila*

by a peak at 24 HPI (53.6%), stabilizing at 71.4% by the end of the experiment (120 HPI) (Fig. 7). This high mortality rate and the debilitated state of fish after 9 HPI limited the feasibility of obtaining consistent transcriptomic data beyond this timepoint.

Discussion

Transcriptome analysis of blood leukocytes from *Piaractus mesopotamicus* during sepsis progression revealed extensive differentiation in gene expression over time. To ensure that the transcriptome analysis accurately reflected the immune response of the leukocytes, erythrocytes were removed prior to RNA-Seq, since in fish as in other vertebrates erythrocytes represent the most abundant fraction of blood cells, accounting for approximately 94% of the total (Ronza et al. 2021). Removing these cells prevented the predominance of genes related to hemoglobin as carriers of oxygen and carbon dioxide (Meitern et al. 2014; Désert et al. 2016), allowing for a more precise assessment of leukocyte gene regulation during sepsis.

The RNA-Seq data demonstrated a highly dynamic immune response, with peak differential gene expression at 3 and 9 HPI, indicating critical immune activation phases. The substantial overlap of upregulated and downregulated genes during these periods suggests intense inflammatory modulation (Chan et al. 2022). Comparative studies show DEG variability depends on tissue type and infection models (Meng et al. 2015; Corral-Lopez et al. 2023). In *A. hydrophila* infections, studies of the spleen (2121 DEGs) (Yang et al. 2016) and liver (4413 DEGs) (Mastrochirico-Filho et al. 2020), the leukocyte analysis detected 17,698 DEGs in the current study, demonstrating broader differential responses than tissue-focused studies.

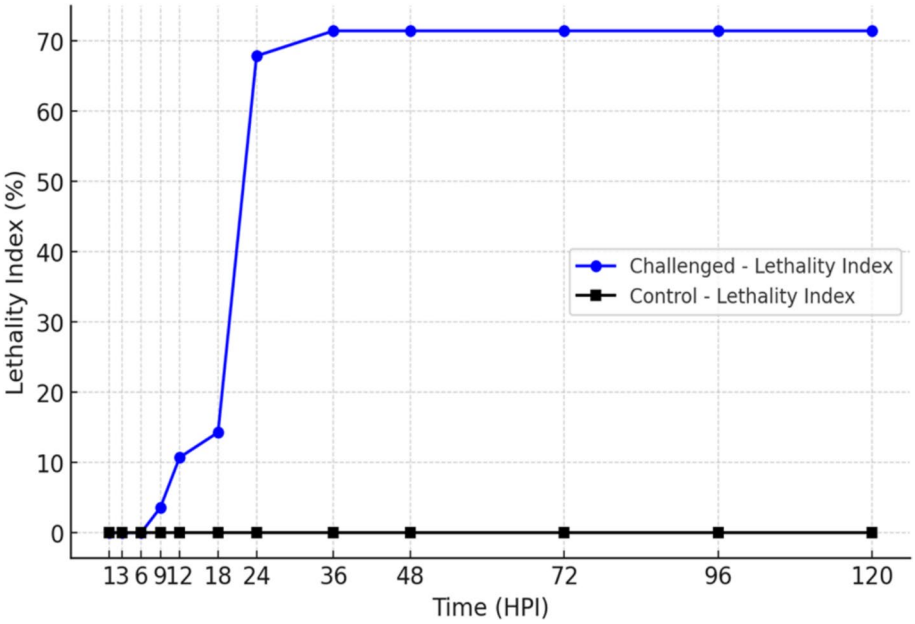

Fig. 7 The lethality index (%), in the challenged group (blue line, circles) and the control group (black line, squares) in pacus during Aeromonosis

Blood leukocytes proved optimal for capturing systemic immune responses, overcoming tissue-specific limitations. Furthermore, the total number of reads after filtering, amounting to 266,272 reads, and the quality of the assembly, with the majority of contigs exceeding 999 bp and an average contig length of 25,695 bp, underscore the reliability of the RNA-Seq technique and the robustness of the adopted approach. This performance contrasts with that reported in studies on Mandarin fish infected by *Flavobacterium columnare*, which yielded an average contig length of only 430 bp (Zhou et al. 2015), and grass carp infected by *Aeromonas hydrophila*, where unigenes averaged 2270 bp (Yang et al. 2016). This enhanced assembly enabled comprehensive transcript coverage, precise isoform identification, and robust functional analysis of the immune response to *A. hydrophila*, establishing leukocytes as a sensitive model for studying host–pathogen interactions.

The leukocyte response to *A. hydrophila* infection was characterized by a highly dynamic process, marked by significant alterations in the transcriptome over time. During the initial phase (1 hpi), there was a predominant downregulation of inflammatory and immune-related genes, including interleukins, interferons, major histocompatibility complex (MHC) molecules, and TNF receptors. Concurrently, an early upregulation of key inflammatory mediators, such as MyD88, tumor necrosis factor (TNF) receptor, and complement system components, was observed, indicative of the prompt activation of inflammatory pathways. Additionally, the elevated expression of heat shock proteins (HSPs) suggests an early cellular stress response, potentially linked to increased vascular permeability, which is critical for facilitating leukocyte migration to peripheral tissues. Notably, the increased vascular permeability in *Piaractus mesopotamicus* has previously been associated with the rapid production of inflammatory mediators, including prostaglandins, leukotrienes (eicosanoids), and pro-inflammatory cytokines such as IL-1β and TNF-α, all of

which play pivotal roles in the early phase of acute inflammation induced by *A. hydrophila* (Claudiano et al. 2019).

The early upregulation of von Willebrand factor expression suggests a significant involvement of hemostasis and cell adhesion in the initial inflammatory response. However, although this factor is expressed early, the associated morphological manifestations such as platelet aggregation, hemorrhagic ascites, thrombosis, and petechial hemorrhages become evident only at later stages of Aeromonosis (6 and 9 hpi) (Marinho-Neto et al. 2019), demonstrating that the initial molecular changes precede observable structural damage.

Peak activation (3 HPI) showed marked upregulation of pro-inflammatory markers, coagulation factors, and lymphocyte activation genes, coinciding with hematological changes—leukocytosis, enhance cell migration, and increased neutrophil, macrophage, and lymphocyte populations at infection sites, corroborating transcriptomic analysis results (Claudiano et al. 2013, 2019) and sustained NF-κB activation. Furthermore, the increased expression of ERO1-like protein suggests enhanced oxidative stress as a key component of the initial pathogen containment mechanism, while the sustained NF-κB pathway activation observed in this study underscores the heightened mediation of pro-inflammatory mediators during *A. hydrophila* sepsis in pacu.

At 6 HPI, emerging regulatory mechanisms (TGF-β) appeared alongside tissue damage markers and iron sequestration strategies (transferrin receptor induction). Morphological and ultrastructural analyses revealed progressively severe tissue damage during this phase, with marked vascular congestion, extensive hemorrhaging, and widespread necrosis particularly affecting liver, spleen, and kidney tissues (Marinho-Neto et al. 2019). Concurrently, upregulated transferrin receptors and iron metabolism genes indicated leukocyte-mediated iron sequestration strategies—a nutritional immunity response that aligned with observed serum biochemical alterations in Aeromonosis (Claudiano et al. 2019).

By the experimental endpoint (9 hpi), the inflammatory response peaked alongside emerging resolution mechanisms, marked by upregulated TGF-β and glucocorticoid receptors. This critical phase coincided with severe tissue damage—including hemorrhagic necrosis, hepatosplenomegaly with vascular congestion, and hemorrhagic enteritis—correlating with initial mortality (Claudiano et al. 2019; Marinho-Neto et al. 2019). Systemic bacteremia (with *A. hydrophila* re-isolation from all tissues) confirmed failed immune containment, while persistent complement system, immunoglobulin, NF-κB, and HSP gene activation indicated sustained inflammatory engagement. Despite metabolic leukocyte preparedness, this ultimately caused catastrophic tissue compromise (Claudiano et al. 2020).

Transcriptomic enrichment analyses revealed that most genes expressed during sepsis were associated with metabolic functions, highlighting the crucial role of biochemical reprogramming in sustaining leukocyte activation during *Aeromonas hydrophila* infection. Specifically, we observed significant upregulation of energy metabolism genes involved in both anaerobic glycolysis and the Krebs cycle, indicating that leukocytes mobilize multiple energy pathways to maintain functionality during sepsis. This metabolic adaptation aligns with previous findings in *Ctenopharyngodon idellus* (Yang et al. 2016; Xiong et al. 2022), and other teleost models of bacterial infection (Yang et al. 2016; Song et al. 2017; Ronza et al. 2021), a conserved host response to systemic bacterial challenge.

Functional analyses (KEGG and GO) revealed that sepsis progression involves complex crosstalk between energy metabolism, ion homeostasis, and inflammatory regulation. The activation of PI3K-AKT, mTOR, and Toll-like receptor (TLR) pathways demonstrates how leukocytes employ adaptive mechanisms not only for direct pathogen combat but also to maintain cellular viability under inflammatory stress (Song et al. 2017; Ronza et al. 2021; Xiong et al. 2022). Notably, previous studies in *A. hydrophila*–infected pacu

specifically implicated the PI3K-AKT pathway in modulating both hepatic and hematopoietic responses, suggesting its dual role in inflammation control and tissue protection (Claudiano et al. 2020; Mastrochirico-Filho et al. 2020).

The sustained activation of steroid hormone pathways indicates a critical endocrine adaptation to systemic inflammatory stress in *P. mesopotamicus*, reflecting significant neuroendocrine and biochemical changes during sepsis. Notably, elevated glucocorticoid production—previously shown to mitigate inflammatory damage and partially restore homeostasis in late-stage *A. hydrophila* sepsis (Claudiano et al. 2019, 2020)—represents a conserved response across teleost species, as confirmed by transcriptomic studies in other pathogenic bacterial infections (Yang et al. 2016; Song et al. 2017; Ronza et al. 2021).

A noticeable finding was the profound reprogramming of iron and calcium metabolism—crucial biochemical mechanisms that limit nutrient availability to pathogens during bacteremia, thereby restricting microbial proliferation (Zhang et al. 2025). The upregulation of transferrin receptors and iron/calcium regulatory genes in advanced sepsis stages aligned with serum biochemical alterations in *P. mesopotamicus* (Claudiano et al. 2019; Mastrochirico-Filho et al. 2020). This nutritional immunity strategy appears evolutionarily conserved among teleosts, as demonstrated by similar transcriptomic responses in *A. hydrophila*–infected grass carp (*Ctenopharyngodon idellus*) and mandarin fish (*Siniperca chuatsi*) (Yang et al. 2016; Song et al. 2017; Ronza et al. 2021; Xiong et al. 2022).

Integrated RNA-Seq, KEGG, and GO analyses reveal that metabolic and neuroendocrine reprogramming lie at the heart of sustaining leukocyte responses during *A. hydrophila*–induced sepsis in *Piaractus mesopotamicus*. Supported by comparative studies, these data uncover a critical interplay among immune activation, energy metabolism, and endocrine regulation, offering new insights into piscine sepsis pathophysiology. This integrated metabolic-immunological response demonstrates how pacu leukocytes prioritize bioenergetic adaptation during acute sepsis without compromising essential immune functions, and underscores how a multi-omics framework provides a robust foundation for developing targeted prophylactic and therapeutic strategies in aquaculture.

KOG analysis revealed a predominance of energy metabolism genes, particularly those involved in amino acid/carbohydrate metabolism and ribosomal biogenesis, highlighting the critical role of metabolic adaptation in sustaining leukocyte function during *A. hydrophila* sepsis. This reprogramming meets the heightened energetic and biosynthetic demands of prolonged inflammation (Yang et al. 2016; Xiong et al. 2022). Concurrent modulation of ion homeostasis (calcium/iron) and transmembrane transport genes further demonstrate leukocyte strategies to maintain intracellular balance while limiting bacterial proliferation. This transcriptional profile conserved across teleost species during systemic bacterial infections (Song et al. 2017; Mastrochirico-Filho et al. 2020; Ronza et al. 2021) underscores the essential role of metabolic flexibility in sepsis progression and immune defense This profile reflects a strategic reallocation of cellular resources during sepsis, where leukocytes prioritize metabolic adaptation and proteostatic maintenance over immunological functions to sustain viability under inflammatory stress and repair DNA suggests a concurrent response to both energetic demands and genotoxic stress during infection.

The inoculation of *A. hydrophila* into the coelomic cavity led to rapid bacterial dissemination through the bloodstream, confirming the development of sepsis in *P. mesopotamicus*, as evidenced by the exclusively positive blood cultures in the challenged groups. Initial mortality was observed at 9 h post-infection (HPI), peaking at 24 HPI (53.6%) and stabilizing at 71.4% by the end of the experiment (120 HPI). This progression confirms the advancement of sepsis and reflects the failure to fully contain the infection, despite the intense metabolic, molecular, and immune adaptations reported

throughout this study. These integrated findings highlight the complex pathophysiology of *A. hydrophila*–induced sepsis in pacus and provide essential insights for future disease control and prevention strategies in aquaculture settings (Claudiano et al. 2019; Marinho-Neto et al. 2019; Mastrochirico-Filho et al. 2020).

The temporal dynamics of transcriptional, metabolic, and structural changes observed in this study reveal that, although leukocytes exhibit an intense mobilization of immune and metabolic pathways to counteract bacterial dissemination, the exacerbated response ultimately leads to significant tissue damage. This is reflected in severe structural lesions, widespread necrosis, and high mortality rates observed at the end of the experimental period (Marinho-Neto et al. 2019). The integration of these findings, from molecular alterations to clinical manifestations, reinforces the value of the leukocyte transcriptome as a sensitive and reliable tool for understanding the pathogenesis of *Aeromonas hydrophila*–induced sepsis. This knowledge contributes to the development of effective therapeutic interventions and prophylactic strategies for the aquaculture of *Piaractus mesopotamicus*.

Conclusion

The integrated analysis of the leukocyte transcriptome revealed that the immune response during *Aeromonas hydrophila*–induced sepsis in *Piaractus mesopotamicus* is highly dynamic and complex. It involves intense metabolic, inflammatory, and neuroendocrine adaptations directly associated with severe clinical manifestations and high mortality rates. These findings enhance our understanding of the pathophysiology of Aeromonosis, highlighting key molecular targets for the development of effective prophylactic and therapeutic strategies in aquaculture.

Supplementary Information The online version contains supplementary material available at https://doi.org/10.1007/s10499-025-02192-5.

Acknowledgements This research was funded by the São Paulo Research Foundation (FAPESP, grant 2014/10231-2) and the National Council for Scientific and Technological Development (CNPq, grant 441054/2014-5).

Author contribution Gustavo S. Claudiano and Larissa A. F. Sampaio conceived and designed the study. Sónia C. S. Andrade, Elaine C. Souza, Jefferson Yunis-Aguinaga, Paulo F. Marcusso, Juliana N. Ferreira, Andrya L. Leão, Thayná M. dos Santos and Layana A. B. Pereira performed the experiments. Laine P. C. dos Santos and Luiz L. Coutinho analyzed the data. Gustavo S. Claudiano and Cleni M. Marzocchi-Machado interpreted the results. Gustavo S. Claudiano drafted the manuscript. Cleni M. Marzocchi-Machado and Julieta R. E. Moraes critically revised the manuscript for important intellectual content. All authors reviewed and approved the final version of the manuscript.

Funding This research was funded by the São Paulo Research Foundation (FAPESP, grant 2014/10231–2) and the National Council for Scientific and Technological Development (CNPq, grant 441054/2014–5). The author was supported by a FAPESP postdoctoral fellowship (grant 2015/12143–6). *In Memoriam*: A Great Friend and Mentor, Professor Flávio Ruas de Moraes.

Data availability All data supporting the findings of this study are provided within the supplementary material. This includes: (i) a complete list of differentially expressed genes (DEGs) across all time points (Supplementary Table S1), (ii) immune-related DEG profiles (Table S2), (iii) Gene Ontology enrichment analysis (Table S3), and (iv) KEGG pathway classification (Table S4). Raw sequencing data (.fastq files) are no longer available due to long-term storage limitations at the time the experiment was conducted.

Declarations

Conflict of interest The authors declare no competing interests.

References

Abeyta C, Kaysner CA, Wekell MM, Stott RF (1990) Incidence of motile aeromonads from United States west coast shellfish growing estuaries. J Food Prot 53:849–855

Ahmed HA, Mohamed MEM, Rezk MM, Gharieb RMA, Abdel-Maksoud SA (2018) *Aeromonas hydrophila* in fish and humans: prevalence, virulotyping and antimicrobial resistance. Slovenian Vet Res 55:113–124

Boyd CE (1990) Water quality in ponds for aquaculture (482 p.). Alabama Agricultural Experiment Station, Auburn University

Chan JTH, Kadri S, Köllner B, Rebl A, Korytář T (2022) RNA-seq of single fish cells – seeking out the leukocytes mediating immunity in teleost fishes. Front Immunol. https://doi.org/10.3389/fimmu.2022.798712

Claudiano GdaS, Petrillo TR, Manrique WG, Castro MP, Loureiro BA, Marcusso PF et al (2013) Acute aerocystitis in *Piaractus mesopotamicus*: participation of eicosanoids and pro-inflammatory cytokines. Fish Shellfish Immunol 34:1057–1062

Claudiano GS, Yunis-Aguinaga J, Marinho-Neto FA, Miranda RL, Martins IM, Otani FS et al (2019) Hematological and immune changes in *Piaractus mesopotamicus* in the sepsis induced by *Aeromonas hydrophila*. Fish Shellfish Immunol 88:259–265

Claudiano GS, Andrade SCS, Souza EC, Yunis-Aguinaga J, Coutinho LL, Moreira DKT et al (2020) Role of neuroendocrine modulation and biochemistry in the sepsis in *Piaractusmesopotamicus*. Gen Comp Endocrinol 288:113338

Corral-Lopez A, Bloch NI, van der Bijl W, Cortazar-Chinarro M, Szorkovszky A, Kotrschal A et al (2023) Functional convergence of genomic and transcriptomic architecture underlies schooling behaviour in a live-bearing fish. Nat Ecol Evol 8:98–110

Debey S, Schoenbeck U, Hellmich M, Gathof BS, Pillai R, Zander T et al (2004) Comparison of different isolation techniques prior gene expression profiling of blood derived cells: impact on physiological responses, on overall expression and the role of different cell types. Pharmacogenomics J 4:193–207

Désert C, Merlot E, Zerjal T, Bed'hom B, Härtle S, Le Cam A et al (2016) Transcriptomes of whole blood and PBMC in chickens. Comparative Biochem Physiol Part D: Genomics and Proteomics 20:1–9

Fan H, Hegde P (2005) The transcriptome in blood: challenges and solutions for robust expression profiling. Curr Mol Med 5:3–10

Goris RJA (1996) MODS/SIRS: result of an overwhelming inflammatory response? World J Surg 20:418–421

Hotchkiss RS, Monneret G, Payen D (2013) Sepsis-induced immunosuppression: from cellular dysfunctions to immunotherapy. Nat Rev Immunol 13:862–874

International Organization for Standardization (2006) Biological evaluation of medical devices — Part 2: Animal welfare requirements — ISO 10993-2:2006

Levy MM, Fink MP, Marshall JC, Abraham E, Angus D, Cook D et al (2003) 2001 SCCM/ESICM/ACCP/ATS/SIS international sepsis definitions conference. Crit Care Med 31:1250–1256

Lévy Y, Sereti I, Tambussi G, Routy JP, Lelièvre JD, Delfraissy JF et al (2012) Effects of recombinant human interleukin 7 on T-cell recovery and thymic output in HIV-infected patients receiving antiretroviral therapy: results of a phase I/IIa randomized, placebo-controlled, multicenter study. Clin Infect Dis 55:291–300

Marinho-Neto FA, Claudiano GS, Yunis-Aguinaga J, Cueva-Quiroz VA, Kobashigawa KK, Cruz NRN et al (2019) Morphological, microbiological and ultrastructural aspects of sepsis by *Aeromonashydrophila* in *Piaractusmesopotamicus*. PLoS ONE 14:e0222626

Mastrochirico-Filho VA, Hata ME, Kuradomi RY, de Freitas MV, Ariede RB, Pinheiro DG et al (2020) Transcriptome profiling of pacu (*Piaractus mesopotamicus*) challenged with pathogenic *Aeromonas hydrophila*: inference on immune gene response. Front Genet. https://doi.org/10.3389/fgene.2020.00604

Meitern R, Andreson R, Hõrak P (2014) Profile of whole blood gene expression following immune stimulation in a wild passerine. BMC Genomics 15:533

Meng X, Tian X, Nie G, Wang J, Liu M, Jiang K et al (2015) The transcriptomic response to copper exposure in the digestive gland of Japanese scallops (*Mizuhopecten yessoensis*). Fish Shellfish Immunol 46:161–167

Ronza P, Álvarez-Dios JA, Robledo D, Losada AP, Romero R, Bermúdez R et al (2021) Blood transcriptomics of turbot *Scophthalmus maximus*: a tool for health monitoring and disease studies. Animals 11:1296

Ross LG, Ross B (2008) Anaesthetic and sedative techniques for aquatic animals, 3rd edn. Wiley-Blackwell

Sarkar A, Saha M, Roy P (2012) Identification and typing of *Aeromonas hydrophila* through 16S rDNA-PCR fingerprinting. J Aquaculture Res Develop 03:2–4

Song X, Hu X, Sun B, Bo Y, Wu K, Xiao L et al (2017) A transcriptome analysis focusing on inflammation-related genes of grass carp intestines following infection with *Aeromonas hydrophila*. Sci Rep 7:40777

Talwar S, Munson PJ, Barb J, Fiuza C, Cintron AP, Logun C et al (2006) Gene expression profiles of peripheral blood leukocytes after endotoxin challenge in humans. Physiol Genomics 25:203–215

Tatusov RL (2000) The COG database: a tool for genome-scale analysis of protein functions and evolution. Nucleic Acids Res 28:33–36

Tatusov RL, Fedorova ND, Jackson JD, Jacobs AR, Kiryutin B, Koonin EV et al (2003) The COG database: an updated version includes eukaryotes. BMC Bioinformatics 4:41

Tavares-Dias M (2006) A morphological and cytochemical study of erythrocytes, thrombocytes and leukocytes in four freshwater teleosts. J Fish Biol 68:1822–1833

Tavares-Dias M, de Moraes FR (2007) Leukocyte and thrombocyte reference values for channel catfish (*Ictalurus punctatus* Raf), with an assessment of morphologic, cytochemical, and ultrastructural features. Vet Clin Pathol 36:49–54

Xiong N-X, Ou J, Fan L-F, Kuang X-Y, Fang Z-X, Luo S-W et al (2022) Blood cell characterization and transcriptome analysis reveal distinct immune response and host resistance of different ploidy cyprinid fish following *Aeromonas hydrophila* infection. Fish Shellfish Immunol 120:547–559

Yang Y, Yu H, Li H, Wang A (2016) Transcriptome profiling of grass carp (*Ctenopharyngodon idellus*) infected with *Aeromonas hydrophila*. Fish Shellfish Immunol 51:329–336

Yunis-Aguinaga J, Fernandes DC, Eto SF, Claudiano GS, Marcusso PF, Marinho-Neto FA et al (2016) Dietary camu camu, *Myrciaria dubia*, enhances immunological response in Nile tilapia. Fish Shellfish Immunol 58:284–291

Zhang R, Li D, Fang H, Xie Q, Tang H, Chen L (2025) Iron-dependent mechanisms in *Acinetobacter baumannii*: pathogenicity and resistance. JAC-Antimicrobial Resistance. https://doi.org/10.1093/jacamr/dlaf039

Zhou W, Zhang Y, Wen Y, Ji W, Zhou Y, Ji Y et al (2015) Analysis of the transcriptomic profilings of Mandarin fish (*Siniperca chuatsi*) infected with *Flavobacterium columnare* with an emphasis on immune responses. Fish Shellfish Immunol 43:111–119

Authors and Affiliations

Gustavo S. Claudiano[1,2,3] · Larissa A. F. Sampaio[1] · Sónia C. S. Andrade[4] · Elaine C. Souza[5] · Jefferson Yunis-Aguinaga[8] · Paulo F. Marcusso[6] · Juliana N. Ferreira[2] · Andrya L. Leão[1] · Thayná M. dos Santos[1] · Layana A. B. Pereira[2] · Laine P. C. dos Santos[2] · Luiz L. Coutinho[7] · Cleni M. Marzocchi-Machado[9] · Julieta R. E. Moraes[3,10]

✉ Gustavo S. Claudiano
gsclaudiano@gmail.com

[1] Institute of Biodiversity and Forests, Federal University of Western Pará, UFOPA, Santarém, Pará, Brazil

[2] Graduate Program in Aquaculture (PPG-AQUI), Nilton Lins University, Manaus, Amazonas, Brazil

[3] Department of Veterinarian Pathology, Faculty of Agrarian and Veterinarian Sciences, São Paulo State University, Unesp, Jaboticabal, São Paulo, Brazil

[4] Department of Genetics and Evolutionary Biology, Institute of Biosciences, São Paulo University, USP, São Paulo, São Paulo, Brazil

[5] Educational Foundation of Penápolis, FUNEPE, Penápolis, São Paulo, Brazil

[6] Faculdade de Medicina Veterinária E Zootecnia da, Universidade Estadual Paulista "Júlio de Mesquita Filho", Botucatu, São Paulo, Brazil

[7] Department of Animal Science, São Paulo University, USP, ESALQ, Piracicaba, São Paulo, Brazil

[8] Universidad Científica del Sur, Lima, Peru

[9] Department of Clinical, Toxicological and Bromatological Analyses, Ribeirão Preto School of Pharmaceutical Sciences, University of São Paulo, USP, Ribeirao Preto, São Paulo, Brazil

[10] Aquaculture Center of UNESP, Caunesp, Jaboticabal, São Paulo, Brazil